Integral descriptors of the vertical structure of the ocean

Francisco Machín and Josep L. Pelegrí

Institut de Ciències del Mar, CSIC, Barcelona, Spain

Running title: Descriptors of the ocean's structure

Corresponding author:

Francisco Machín (fmachin@icm.csic.es)

Passeig Marítim de la Barceloneta, 37–49,

08003 Barcelona (Spain)

Abstract

We propose a simple polynomial expression for neutral density and nutrients as a function of potential temperature, pressure and salinity. The expression is applied to the 1988 North Atlantic A16 WOCE meridional section and the polynomial coefficients are calculated using an inverse technique. The resulting polynomials show good skill in reproducing the nutrients and density structure, as verified through an analysis of variance (ANOVA) test. The large-scale changes in the polynomial coefficients occur between equatorial (E), tropical (T), subtropical (ST), and subpolar (SP) waters. The temperature and pressure coefficients experience substantial changes at all transitions (E-T, T-ST, and ST-SP), while the salinity ones only have major variations at the T-ST transition. Mesoscale-like oscillations occur all along the section but are relatively small, except between about 40 and 50°N, in a region of rough bottom topography. The density field is reconstructed using individual and group coefficients, and the contribution of each coefficient is identified. The method is also applied to analyze the neutral density distribution in a nearly identical 2003 section, removing near-surface density values that may be related to different warming/cooling of the surface layer. The results show close resemblances but also some significant variations, which are discussed in terms of interdecadal variability. Hence, we argue that the set of calculated coefficients provides good integral descriptors for the vertical structure of the ocean.

Keywords: inverse model, WOCE A16 section, nutrients, neutral density, water mass, interdecadal changes, ocean descriptor.

1 Introduction

Oceanographers are faced with the task of finding simple descriptors for the complex temporal and spatial changes in the structure of the ocean. Large-scale variations, for example, are commonly described in terms of water masses, which result from atmospheric forcing over a significant portion of the ocean. The water-type concept is used to characterize each water mass with just a few temperature and salinity pairs, in essence providing a descriptor of the ocean's response to the forcing mechanisms.

Our aim here is to use an inverse model, inspired by standard property-property diagrams, to obtain such integral descriptors of the thermodynamic structure of the ocean. Inverse models are skillful at estimating the best possible parameters that adjust geophysical models to actual observations, hence becoming a synthesis tool. In oceanography these models have been used in different cases, as in acoustic tomography (Munk and Wunsch, 1979) and in general circulation (Wunsch, 1977). Nevertheless, to our knowledge they have not yet been applied to objectively determine simple descriptors for the ocean's vertical structure.

The fundamental idea is to use a simple relation for one dependent variable as a function of several independent hydrographic variables, either thermodynamic or chemical-biological variables. The relation becomes a geophysical model and its coefficients, which change in time and space, are integral parameters that respond to the ocean's internal organization. If the relation is left simple enough, then its predictive skill rests on the coefficients' (spatial and temporal) variability.

The desired simplicity contrasts with other examples of geophysical models, such as the equation of state (density ρ as a function of temperature T, pressure p, and salinity

S). Another example is neutral density γ, where the compressing effect of pressure is fully removed (McDougall, 1987; Jackett and McDougall, 1997). Neutral density is expressed in terms of three fully independent variables, S, p and potential temperature (θ), in the sense that a process leading to changes in one of the three variables would not produce modifications in the other two. In both examples the geophysical model is very complex: it has full predictive skill, as it describes the ocean as composed of infinite possible states, but zero descriptive content.

Here we test the descriptive content of simple models for three nutrients (nitrates N, phosphates P, and silicates Si) and neutral density γ (henceforth simply referred as density). The models for the dependent variables are linear polynomial expressions as a function of the triad (θ, p, S). The coefficients are chosen to minimize the difference between observations and predictions. They change smoothly with horizontal coordinates (hereafter stations or positions, characterized by one oceanographic station), restrained by weights imposed from oceanographic information. Hence, the polynomial becomes a simplified model for the ocean and the values of the coefficients are characteristic of its structure at each position. As this structure depends on the large-scale dynamics, we expect that changes in the coefficients should be indicative of variations in the forcing mechanisms and the ocean's internal organization.

In the next section we briefly describe the data sets selected to test the model. In Section 3 we explain the main details of an inverse model, proposed as a tool to obtain simple descriptors of the ocean structure, emphasizing the importance of the proper selection of a reference level. In Section 4 we apply the method to the WOCE A16N section and present the main results, while in Section 5 we analyze the model's skill at reproducing

the observations, with special attention to the significance of the coefficients. In Section 6 we apply the model to two realizations of the same section, taken 15 years apart, and briefly discuss the observed changes, and in Section 7 we presents the conclusions.

2 Data

In order to test the model we have selected the eastern North Atlantic A16 WOCE meridional section (Figure 1), which consists of 116 casts down to the sea floor taken between the Equator and 64°N in July-August 1988, roughly along 20°W (Tsuchiya et al., 1992). A16N WOCE section was revisited in June-August 2003, occupying nearly exactly the same locations as in the 1988 cruise (Johnson et al., 2005). The temperature, salinity and nutrients data for both sections are available from the Clivar and Carbon Hydrographic Data Office. The number of observations used to determine the coefficients changes with the depth of the station and also depends on the variable considered (i.e., density or nutrients). For deep stations there are roughly 500 observations for density (values are averaged over 10 m depth intervals) and some 24 nutrient observations along the water column, so the coefficients are obtained using very different numbers of equations (between about 24 and 500).

The panels in Figure 2 present the meridional distribution of potential temperature, salinity, density and nutrients as a function of depth. The isothermals (top left panel) and isohalines (middle left panel) illustrate the presence of several transition bands in the upper-ocean. A low-latitude band is located roughly at 6-10°N, at about the location where the upper-ocean's isothermals and isohalines rise, linked to the North Equatorial Counter-Current, in the equatorial-tropical transition (E-T) (Stramma and Schott, 1999).

A middle-latitude band is found between about 15 and 20°N, where the S and θ isolines sink in association with the North Equatorial Current, just north of the Cape Verde frontal zone, in what constitutes the tropical-subtropical margin (T-ST) (Zenk et al., 1991). Finally, a high-latitude band is found after the shallow summits around 42-50°N, near the subtropical-subpolar margin (ST-SP) (Tsuchiya et al., 1992; Lozier et al., 1995). On the other hand, the isoneutrals (third left panel) are fairly horizontal in the tropical and subtropical ocean, from the Equator to 30°N, down to about 3000 m. Major slopes, reflecting the formation of deep-waters, are found only in the subpolar gyre ($>$ 42°N) waters.

The right three panels in Figure 2 display the nitrate, phosphate and silicate distributions. All nutrients are depleted at the sea surface by biological consumption. Nitrates and phosphates have similar distributions, with both nutrients increasing up to a subsurface maximum. In the subtropical and subpolar gyres this maximum occurs in the nutrient bearing stratum (e.g. Pelegrí and Csanady, 1991), at depths of 600-800 m within North Atlantic Central Waters (NACW), and in equatorial and tropical waters as a tongue of Antarctic Intermediate Water (AAIW) located at some 800-900 m depth (e.g. Machín et al., 2006). The intrusion of Antarctic Bottom Water (AABW) is the cause of a second deep maximum, below 4000 m depth (e.g. Holfort and Siedler, 2001). In contrast, silicates present a rather different distribution along the water column, with a continuous increase below 2000 m depth, so that the AAIW and AABW tongues do not stand out as much as those for nitrates and phosphates. All panels in Figure 2 are characterized by the presence of substantial mesoscale-like fluctuations between about 38 and 52°N, apparently associated with the rough bottom topography in this region.

3 Inverse model

3.1 Polynomial relation

As mentioned in the Introduction, we explore the following model:

$$\begin{aligned} I &= a_0 + a_1(\theta - \theta_r) + a_2(\theta - \theta_r)^2 + ... + a_l(\theta - \theta_r)^l + \\ &+ b_1(p - p_r) + b_2(p - p_r)^2 + ... + b_n(p - p_r)^n + \\ &+ c_1(S - S_r) + c_2(S - S_r)^2 + ... + c_m(S - S_r)^m, \end{aligned} \tag{1}$$

where I is the dependent variable, either density or nutrient concentration. The polynomial coefficients are a_i, b_i, and c_i, and the order of the polynomial is set by l, n and m. The independent variables are taken relative to some reference potential temperature θ_r, pressure p_r and salinity S_r reference levels, and their specification is discussed in the next section.

We want the polynomial degree to be a compromise between simplicity and predictive skill. For this purpose we have explored, for all dependent variables, all possible combinations of polynomial degrees on θ, p, and S varying from zero to six. For each case we have used an ANOVA test to evaluate how much of the total variability (TV) in the observations along the A16 line is explained by the variability between simulations (VBS) and the variability within each simulation (VWS). We base our choice on the values given by the adjusted-R^2 (R_a^2), defined as the ratio between the variability explained by each simulation and the total variability in γ:

$$R_a^2(l, n, m) = \frac{VBS}{TV} \frac{N - 1}{K - 1} \tag{2}$$

where N is the number of observations and K is the number of cases considered.

Figure 3 shows the R_a^2 distribution for density and nutrients as a function of the order of the polynomial: (l, n, m) for (θ, p, S). In all cases, high polynomial degrees are needed for one single variable to obtain a high R_a^2, while the degrees are drastically reduced after combining variables. For example, in the central panel (upper row) we observe that on its own θ needs a sixth degree to explain 0.998 of the γ variability, while for this same degree salinity on its own only explains 0.95 of the variability. However, when both variables are allowed to work together, a variability above 0.999 is achieved for $l = 2$ and $n = 1$ (while maintaining $m = 0$). Similar results are obtained for the nutrient polynomials, with the skill at predicting nutrient variability improving rapidly as we move from one to three independent variables.

Following the simplicity *versus* predictability compromise, we use a model that predicts each dependent variable (density or any nutrient) through a second degree polynomial on all three independent variables, $l = m = n = 2$. Such a set of degrees is capable of explaining nearly 100% of the variability in either dependent variable. Hence we express I by a second order polynomial function on θ, p and S as

$$I = a_0 + a_1(\theta - \theta_r) + a_2(\theta - \theta_r)^2 + b_1(p - p_r) + b_2(p - p_r)^2 + c_1(S - S_r) + c_2(S - S_r)^2. \quad (3)$$

Expression (3) is applied to observations from the sea surface to the bottom, along constant pressure levels. It can be written in matrix form as $\mathbf{I} = \mathbf{E}\mathbf{x} + \mathbf{r}$, where $\mathbf{x}$ contains the model coefficients and $\mathbf{r}$ considers the model residuals, the latter induced by noise in the observations and inaccuracies in the model formulation. This expression constitutes a grossly overdetermined system and its solution is obtained by a fit in a least squares sense. A weighted tapered least squares adjustment is used to minimize the residuals (Menke, 1984; Wunsch, 1996). Weights incorporate oceanographic information

and constrain the system to produce a solution coherent with the *a priori* information. This is done in two ways: (1) by making each polynomial term produce a similar response in the dependent variable; and (2) by taking into account the variability of the dependent variables (estimated as the standard deviation in the observations) at each pressure level, i.e. the importance of each equation is inversely proportional to the dispersion of the corresponding density or nutrient concentration at that level.

3.2 Reference level

In the model we have added physical content by introducing reference variables (θ_r, S_r and p_r), as if we were examining how much the different points in the water column deviate from some reference state. The reference variables are those that define the reference neutral density $\gamma_r \equiv \gamma(\theta = \theta_r, p = p_r, S = S_r)$, i.e. $\theta_r(x, y) \equiv \theta(\gamma = \gamma_r)$, $p_r(x, y) \equiv p(\gamma = \gamma_r)$, and $S_r(x, y) \equiv S(\gamma = \gamma_r)$. In this way each independent variable corresponds to the deviation from a reference value and if the model has perfect predictability, i.e. equation (3) becomes an identity for all observations, then $a_0 = \gamma_r$.

The selection of γ_r is a key aspect of the model, as it determines the reference levels in the inverse model. A physically meaningful γ_r should embrace one single water mass, with roughly constant potential temperature and salinity values. The independent polynomial coefficients hence become the variables that specify the characteristics of this water mass.

Strictly speaking we should use an analogous procedure to get references values for each nutrient. In contrast to density, however, these variables are not uniquely defined at each position, as a given value of nutrient concentration may be found in more than one level in the water column. Hence, we have maintained the same reference values

as those obtained by setting a density reference. This sets some reference nutrients, $N_r(x,y) \equiv N(\gamma = \gamma_r)$, $P_r(x,y) \equiv P(\gamma = \gamma_r)$, and $Si_r(x,y) \equiv Si(\gamma = \gamma_r)$, which must be checked for consistency.

As a sensitivity test we examine how the coefficients and reference variables vary as a function of the selected reference density, for each station, by running the inverse model with reference densities spanning the water column from the sea surface to the sea floor. Figure 4 shows the meridional distribution of the reference variables and polynomial coefficients obtained for predicting density. Both θ_r and S_r respond to the different water masses from the equator to the subpolar gyre. A reference level in central ($\gamma_r < 27.3$) and intermediate waters ($27.3 < \gamma_r < 27.9$) produces substantial changes in the reference variables, while deep waters ($\gamma_r > 27.9$) induce much less variability. For instance, the effect of the northward penetrating Antarctic Intermediate Water can be observed at lower latitudes centered on $\gamma_r = 27.5$, as it induces relatively low S_r values. Likewise, the presence of Mediterranean Water clearly affects both θ_r and S_r in the region from 20°N to 40°N, as it induces relatively high θ_r and S_r. This contrasts with a reference density located within deep waters, characterized by one single water mass, which results in little variations of the reference variables.

Figure 4 also shows the meridional dependence of the density coefficients on the reference-density selection. As expected, a_0 remains near constant latitudinally for any given reference density. The lineal coefficients a_1 and c_1 show significant variations with both reference-density and latitude, while the main dependence of b_1 is on latitude. All quadratic coefficients (a_2, b_2 and c_2) only change significantly with latitude.

Figure 5 presents the meridional and depth distribution of the thermal expansion

and salinity contraction coefficients, respectively defined as $\rho\alpha \equiv -\partial\rho/\partial\theta|_{S,p}$ and $\rho\beta \equiv \partial\rho/\partial S|_{\theta,p}$. Changes in these expansion coefficients are significant throughout the WOCE section, with similar patterns but different signs, reflecting their opposite effect on density. It may be appreciated that a_1 and c_1 (Figure 4) have absolute values that are similar (but not equal) to the depth-mean values of $\rho\alpha$ and $\rho\beta$, respectively. The fact that the polynomial coefficients differ from the depth-mean expansion coefficients is an expected result, as the inverse model processes much more information than just a simple depth-average; nevertheless, the similarity gives confidence about the model's good behavior.

A second simple sensitivity test for the model is carried out by changing the density variability from 0.1 to 10 times the standard deviation at each pressure level. We find that the inverse solution is very robust as the reference values and coefficients depend little on this selection, with variations nowhere greater than 10% (not shown).

When using the polynomials to retrieve the independent variable, we find that observations are always well reproduced, regardless of the reference density used. The absolute value of the difference between observations and predictions has a near-surface maximum of 0.03 kg m^{-3} but its mean-depth standard deviation is much smaller, ranging between 0.0002 kg m^{-3} and 0.0010 kg m^{-3}.

Following the above sensitivity calculations, hereafter we use the polynomials with a reference density $\gamma_r = 28.072$, which is located in the deep water masses at nearly 3000 m. We skip those shallow stations that do not reach this value, most of them located between 52 and 58°N. For these stations we would require a shallower reference density but, in a long transoceanic section, such a level would not meet the criterion of belonging to one single water-mass.

4 Results

4.1 Coherence tests

To assess the goodness of the model we first check for geometrical coherence in the density results. A plot of neutral density as a function of one variable (θ, p, or S) would immediately suggest the sign of the lineal (slope) and quadratic (curvature) coefficients. With this check in mind we run the inverse model for three different cases, using the data from all stations. In each case we use a second-order polynomial to examine the dependence on one single variable. In the first case a_0, a_1 and a_2 are calculated but all other lineal and quadratic coefficients are set to zero; in the second case a_0, b_1 and b_2 are the calculated variables; and in the last case the system is solved only for a_0, c_1 and c_2. The results obtained this way are coherent with the geometrical interpretation (Figure 6). Relatively large absolute values of the lineal coefficient (e.g. negative a_1) indicate high stratification with respect to the corresponding variable (θ) as a result of the influence of the other two variables (p and S). Similarly, the quadratic coefficient indicates whether the stratification in the corresponding variable is relatively high at deep (e.g. negative a_2) or shallow (positive a_2) density levels.

The good behaviour of the model is also reflected by the reference values of the independent variables, θ_r, p_r and S_r, (Figure 7) as well as by the nutrient reference values, N_r, P_r and Si_r (Figure 8). The independent reference variables are roughly constant, with θ_r and S_r slowly increasing with latitude, and p_r remaining nearly constant at 3000 m until about 52°N, where the reference density finds the sea floor. The nutrient concentrations at the reference density level decrease significantly with latitude, from tropical to subpo-

lar regions, due to the influence of AABW (Figure 2). The independent coefficients for nutrients remain close to the corresponding reference levels, hence validating the method used for the selection of these levels.

4.2 Density coefficients

Figure 8 shows the latitudinal distribution for the reference variables and coefficients, now obtained from the full density model, for $\gamma_r = 28.072$. The constant coefficient a_0 remains everywhere very close to the selected γ_r. The lineal and quadratic coefficients are substantially modified from the above geometrical check cases, in some cases even changing sign. All coefficients display smooth, large-scale trends, with some minor short-scale ($1 - 2^\circ$ latitude) variations. Three major transition bands may be identified, which appear related to the potential temperature and salinity distributions in the upper-ocean (Figure 2). A low-latitude band is located in the E-T transition, a middle-latitude band is found in the T-ST margin, and a high-latitude band is found at about the ST-SP limit.

All coefficients for the density model display substantial changes at both the E-T and T-ST transitions (the changes in the pressure coefficients are less clear because of the compressed vertical axis, as a consequence of including the shallow northern waters). In contrast, the ST-SP transition becomes evident only in the salinity coefficients (c_1 and c_2). The subtropical gyre displays remarkable behaviour in the salinity coefficients (c_1 decreases and c_2 increases) which is not visible in the coefficients for the other variables, and which might possibly be related to the major influence of the Mediterranean Water outflow. Finally, the ST-SP transition zone also displays mesoscale-like variability, most visible in the potential temperature coefficients and probably linked to the rough

topography.

4.3 Nutrient coefficients

Figure 8 also shows the results for all three nutrients. The constant coefficients derived from the nutrient models decrease with latitude, closely following the reference nutrient concentrations. Changes in the lineal and quadratic coefficients may be related to the presence of transition bands in the nutrient distributions (Figure 2), as discussed in reference to density. The latitudinal variability is similar for N and P. Bands E-T and T-ST appear in all coefficients but c_2, which only contains the T-ST band. ST-SP band is present in the a_1, a_2, b_1 and b_2 coefficients. For Si the situation is quite different: the E-T transition band is observed for a_1 and c_1 coefficients, while the T-ST and ST-SP transitions occur in the three linear coefficients (a_1,b_1, and c_1). A similar latitudinal variability is observed for a_1 and b_1, anticorrelated with a_2 and b_2, respectively.

The analogous behaviour of the N and P coefficients, in contrast to the Si ones, is a coherent result given the close correspondence in the cycles of these nutrients. This supports the idea that the calculated coefficients are good integral descriptors of the structure of the water column.

5 Model skill: partial and full reconstructions

Figure 9 shows the differences between neutral-density observations and predictions, as a function of pressure, as reconstructed with the polynomial coefficients shown in Figure 8. As a reference, in the left panel we also show the standard deviation from the mean density at each pressure level. This deviation is maximum in the surface mixed-layer,

0.03 kg m^{-3}, and decreases from 10^{-2} to 10^{-6} kg m^{-3} with depth. The accuracy of the model, or difference between predictions and observations, is typically one order of magnitude better than the standard deviation in the density variations. Similar results are obtained for nutrients (not shown).

Once we have obtained a set of reference variables and polynomial coefficients, we may wonder about the relative importance of each coefficient on the solution. Figure 10 presents eight different density reconstructions on section A16N, in all cases with a mean density (obtained using the latitudinal-mean coefficients and reference variables) as the vertical axis. The figure has been prepared to visualize the role played by each individual term of the polynomial expansion, i.e. each panel shows whether the density predicted using a particular set of local coefficients is greater or less than that expected from the mean coefficients. In the upper-right panel the density is obtained using all local coefficient and reference values, i.e. to obtain the best possible reconstruction. Within the remaining rows, in the left and center panels the density is calculated using the latitudinal mean coefficients and reference values except for the indicated polynomial term, for which both the coefficient and the corresponding reference variable are allowed to change with latitude. In the remaining right panels we have respectively used the independent term a_0 plus all potential temperature (a_i), pressure (b_i), and salinity (c_i) coefficients. Note that in all cases the coefficients are those calculated using the full model.

The individual and group reconstructions evidence the existence of the E-T, T-ST and ST-SP transitions described above. The full reconstruction (upper-right panel) shows the presence of the E-T and T-ST transitions in the upper ocean, characterized by the shallowing isoneutrals. It also illustrates that the intermediate isoneutrals shallow until

some latitude within the subtropical gyre (about 35°N), from where they deepen again. The deep waters remain quite independent of latitude.

The remaining reconstructions are very informative about the role played by an individual coefficient, or group of coefficients. The E-T and T-ST transitions are clearly reflected in the lineal temperature and salt coefficients (a_1 and c_1) and, to a lesser degree, in the quadratic temperature and salinity ones (a_2 and c_2). The ST-SP transition appears to be mainly associated with both lineal and quadratic pressure and salinity coefficients, with the pressure ones reproducing the reduced stratification at high latitudes.

The northern subtropical waters and the ST-SP transition zone are characterized by small mesoscale-like changes associated with all coefficients. This occurs at all depths, but most clearly in the upper and intermediate water strata. These oscillations may be related to the presence of Mediterranean Water outflow within the subtropical gyre and the rough bottom topography in the transition zone.

6 Tool for assessing temporal variability

In order to asses the impact of the surface mixed-layer on the latitudinal variability of the coefficients, we have re-analyzed the data but now discarding observations with density less than 26.85 (roughly in the upper 50 to 200 m, see Fig. 2). The new set of coefficients (Figure 11, left panels) have latitudinal changes which are similar to those obtained from observations spanning the entire water column, in particular identifying the same transition bands (Figure 8). Despite this, there are some differences which indicate that different surface waters may have an impact on the coefficients.

The above result shows that removal of data from surface layers, which are subject to

seasonal variations, becomes essential if we wish to use the method to assess long-term, e.g. interannual or interdecadal, variability in the structure of the ocean. This is true even if we want to compare hydrographic sections obtained during the same season, in different years, as the surface mixed-layer is prone to rapid variations that result from changes in atmospheric forcing.

To illustrate the method's potential for studying long-term variability, we have applied it to the density distribution corresponding to the 2003 A16N homologous cruise, again removing data with densities less than 26.85 (Figure 11, right panels). From Figure 11 we appreciate that applying the inverse model to both realizations (1988 and 2003) leads to coefficients that, as expected, have similar distributions. However, there are some significant differences that deserve special attention.

Figure 12 presents a comparison of the density data and calculated coefficients between both realizations. The top panel shows the density-difference distribution, calculated as the 1988 value subtracted from the 2003 one. The largest neutral density changes, above 0.1, occur at high latitudes, north of roughly 35°N, with a generalized increase of density in the top 700-800 m and alternation of positive and negative values between these depths and some 1500 m. At lower latitudes changes are always less than 0.1 except in the tropics, where the near-surface waters have increased their density.

The subsequent panels in Figure 12 illustrate the relative difference in the coefficients, calculated as the 2003 value minus the 1998 value divided by the latter. As the absolute value of coefficients changes substantially with latitude, it is this relative difference, rather than the absolute one, that will tell us where significant changes are taking place. Since pairs of coefficients are associated with different variables (a_1 and a_2 with potential

temperature, b_1 and b_2 with pressure, and c_1 and c_2 with salinity), changes in their values may be interpreted as indicative of the contributions of these variables to density changes.

The relatively large changes in the salinity coefficients appear to be related to variations in freshwater content between the late 1980s and the early 2000s in the North Atlantic. Freshening has occurred in the whole water column north of about 45°N, which is reflected in the c_1 values, while salinification has happened in the permanent thermocline of subtropical and tropical regions (Boyer et al., 2005), with major changes in c_2 at about 40°N (top 1500 m) and between 10 and 20°N (down to some 800 m).

In the North Atlantic major warming has also occurred during these same periods (Boyer et al., 2007). Between the late 1980s and the end of the millennium, warming was greatest in the subtropical and tropical waters, while cooling was restricted to latitudes around 60°N (Johnson et al., 2005; Levitus et al., 2005). These changes may be reflected in the distributions of the temperature coefficients, which experience large changes in the subpolar (above 45°N) and tropical (less than 20°N) latitudes. In particular, variations are clear at latitudes less than 10°N and between 15 and 20°N, but are simultaneous with pressure coefficients, suggesting that in these regions temperature changes are associated with both meridional and vertical displacements of the isotherms. However, the increase in near-surface density between 3 and 5°N seems to be related solely to temperature changes.

Between 20 and 25°N the pressure coefficients display changes that are larger than the relative changes in the other two sets of coefficients, and have little effect in the density values. This is the position of the Cape Verde frontal zone, a density compensating region that experiences substantial lateral intrusions (e.g. Pastor et al., 2008). These

intrusions imply depth changes in the position of water masses, while the temperature-salinity relation remains unmodified.

7 Conclusions

We diagnose the state of the ocean in terms of a set of polynomial coefficients. In this manner each horizontal position is characterized by a set of coefficients, which become integral descriptors of the ocean's vertical structure. The main virtue of the model here presented is its skill in reproducing the density structure, with smooth variations in the coefficients as we move between adjacent stations. The model is extended to nutrient observations and shows that nitrate and phosphate, which have similar biochemical behavior, produce coefficients with comparable latitudinal variability, while silicate leads to quite different latitudinal patterns. This suggests that the polynomial coefficients respond to the internal organization of the ocean as described by any of those variables (neutral density and biochemical tracers), and that their values have true physical significance. In the case of neutral density the coefficients are related but not equal to mean-depth averages of classical thermodynamic variables such as the thermal expansion coefficient and the saline contraction coefficient.

The size of the lineal coefficient responds to the degree of stratification with respect to the corresponding variable, e.g. a large-negative a_1 indicates large stratification with θ, as a result of the influence of the other two independent variables. Similarly, the sign and magnitude of the quadratic coefficient indicates how much and where the stratification occurs as a function of the corresponding variable, e.g. a large-positive a_2 indicates that the upper/lower portion of the water column is strongly/weakly stratified with θ, as

induced by the other variables. Further work, particularly with sections through frontal regions, is required to improve our understanding of the coefficients' significance and how they depend on the choice of reference neutral-density.

The methodology may be applied to different dependent variables, such as chemical or biological ones, as shown for nutrients. It could also be extended to different domains, e.g. by replacing the dependence on depth z with dependence on latitudinal distance y and doing the analysis at different depth-positions. In the North Atlantic, where at depth we find water masses generated at high latitudes, we could expect that the depth and latitudinal coefficients would have similar patterns.

The potential of the methodology relies on its capacity for classifying an oceanic region in terms of a set of coefficients. To illustrate this potential we present an application to the A16N WOCE meridional line, which was carried out in 1988 and the transect repeated in 2003. The results show the existence of substantial changes in the values of the coefficients, which are in conformity with studies of interdecadal variability in the North Atlantic.

Acknowledgements

We thank WOCE for making available the hydrological data set. This work has been carried out with support from the CANOA Project (CTM2005-00444/MAR), funded by the Spanish Ministerio de Educación y Ciencia. The first author wishes to acknowledge funding through the Juan de la Cierva Programme. We would also like to thank two anonymous reviewers as their comments have helped to greatly improve the final version

of the manuscript.

References

Boyer, T., S. Levitus, J. Antonov, R. Locarnini, A. Mishonov, H. Garcia, and S. A. Josey, 2007: Changes in freshwater content in the North Atlantic Ocean 1955-2006. *Geophys. Res. Lett.*, **34**, L16 603.

Boyer, T., S. Levitus, J. I. Antonov, R. A. Locarnini, and H. Garcia, 2005: Linear trends in salinity for the World Ocean, 1955-1998. *Geophys. Res. Lett.*, **32**, L01 604.

Holfort, J. and G. Siedler, 2001: The meridional oceanic transports of heat and nutrients in the South Atlantic. *J. Phys. Oceanogr.*, **31**, 5–29, 373.

Jackett, D. and T. McDougall, 1997: A neutral density variable for the world's oceans. *J. Phys. Oceanogr.*, **27**, 237–263, 202.

Johnson, G. C., J. L. Bullister, and N. Gruber, 2005: Labrador Sea Water property variations in the northeastern Atlantic Ocean. *Geophys. Res. Lett.*, **32**, L07 602.

Levitus, S., J. Antonov, and T. Boyer, 2005: Warming of the world ocean, 1955-2003. *Geophys. Res. Lett.*, **32**, L02 604.

Lozier, M. S., W. B. Owens, and R. Curry, 1995: The climatology of the North Atlantic. *Prog. Oceanog.*, **36**, 1–44, 180.

Machín, F., A. Hernández-Guerra, and J. L. Pelegrí, 2006: Mass fluxes in the Canary Basin. *Prog. Oceanog.*, **70 (2-4)**, 416–447.

McDougall, T., 1987: Neutral surfaces. *J. Phys. Oceanogr.*, **17**, 1950–1964.

Menke, W., 1984: *Geophysical Data Analysis: Discrete Inverse Theory.* Academic Press, INC., Orlando, 260 pp., 46.

Munk, W. and C. Wunsch, 1979: Ocean acoustic tomography, a scheme for large scale monitoring. *Deep-Sea Res.*, **26**, 123–161.

Pastor, M., J. Pelegrí, A. Hernández-Guerra, J. Font, J. Salat, and M. Emellanov, 2008: Water and nutrient fluxes off Northwest Africa. *Cont. Shelf Res.*, **28 (7)**, 915–936.

Pelegrí, J. L. and G. T. Csanady, 1991: Nutrient transport and mixing in the Gulf Stream. *J. Geophys. Res.*, **96 (C2)**, 2577–2583, 440.

Stramma, L. and F. Schott, 1999: The mean flow field of the tropical Atlantic Ocean. *Deep-Sea Res. II*, **46**, 279–303.

Tsuchiya, M., L. Talley, and M. McCartney, 1992: An eastern Atlantic section from Iceland southward across the Equator. *Deep-Sea Res.*, **39 (11/12A)**, 1885–1917, 145.

Wunsch, C., 1977: Determining the general circulation of the oceans: a preliminary discussion. *Science*, **196**, 871–875, 313.

Wunsch, C., 1996: *The ocean circulation inverse problem.* Cambrige University Press, 442 pp.

Zenk, W., B. Klein, and M. Schröder, 1991: Cape Verde Frontal Zone. *Deep-Sea Res.*, **38 (Suppl.1)**, 505–530, 467.

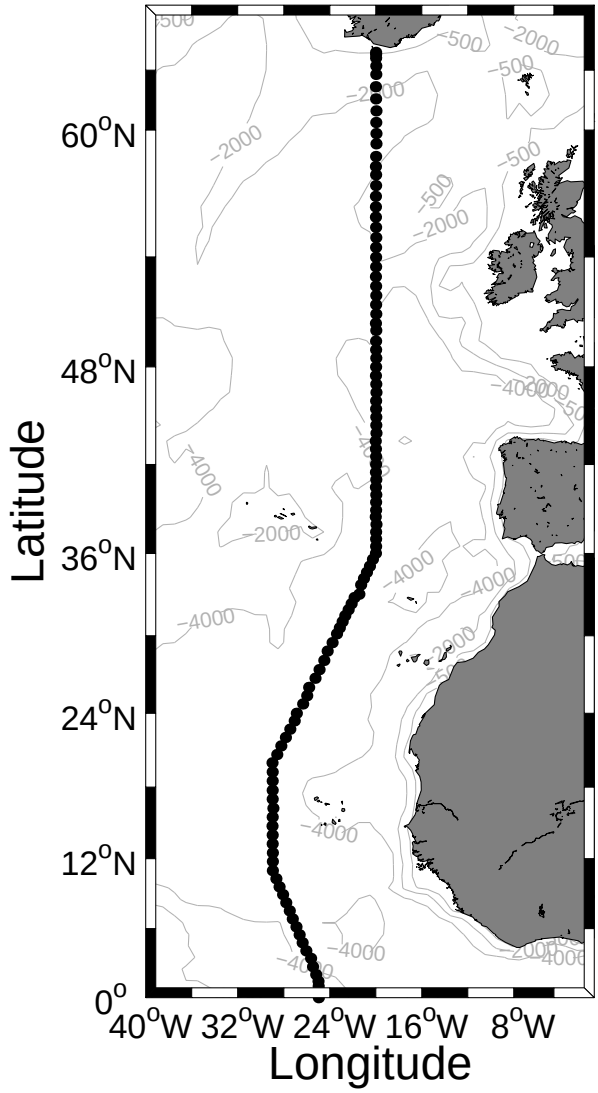

Figure 1: A16N WOCE line, from the Equator to Iceland along the eastern North Atlantic.

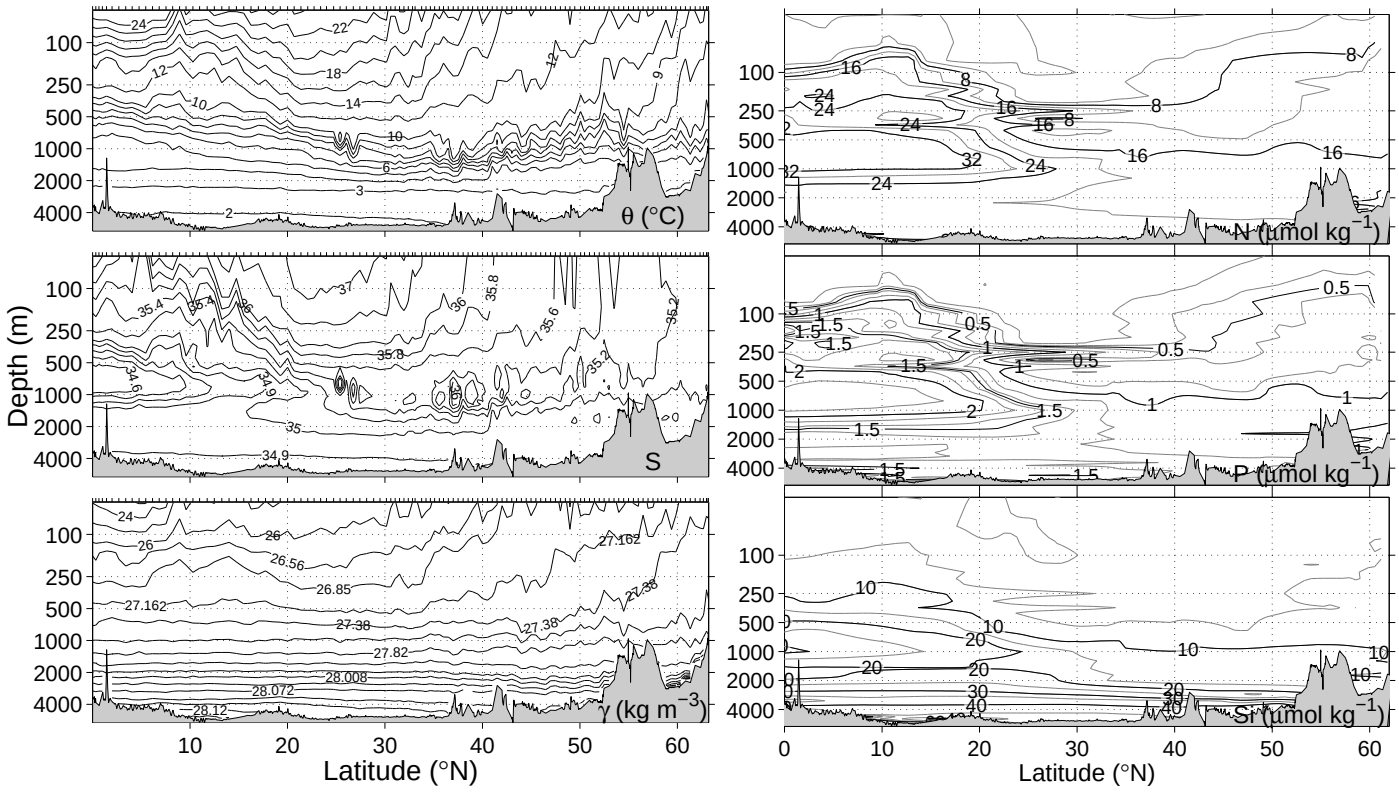

Figure 2: Vertical sections of θ, S, γ, N, P and Si along the A16 WOCE cruise from the Equator to Iceland.

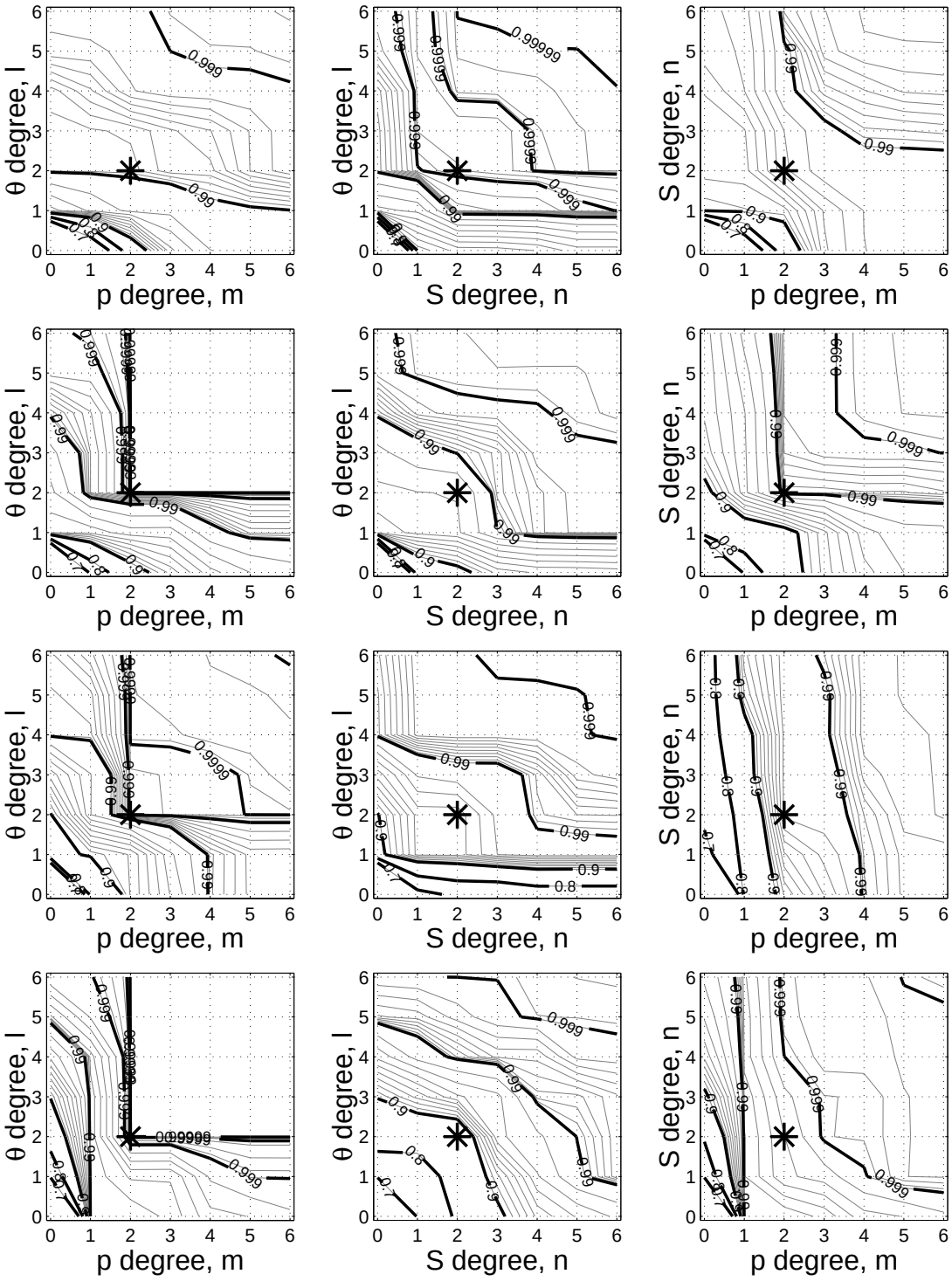

Figure 3: Adjusted R^2 for γ (upper row) and nutrient models (second row corresponds to nitrates, third to phosphates and lower row to silicates) as a function of the degree of the independent variables (l, m and n). Each panel shows the dependence on the order of two variables, while the third variable remains of order zero.

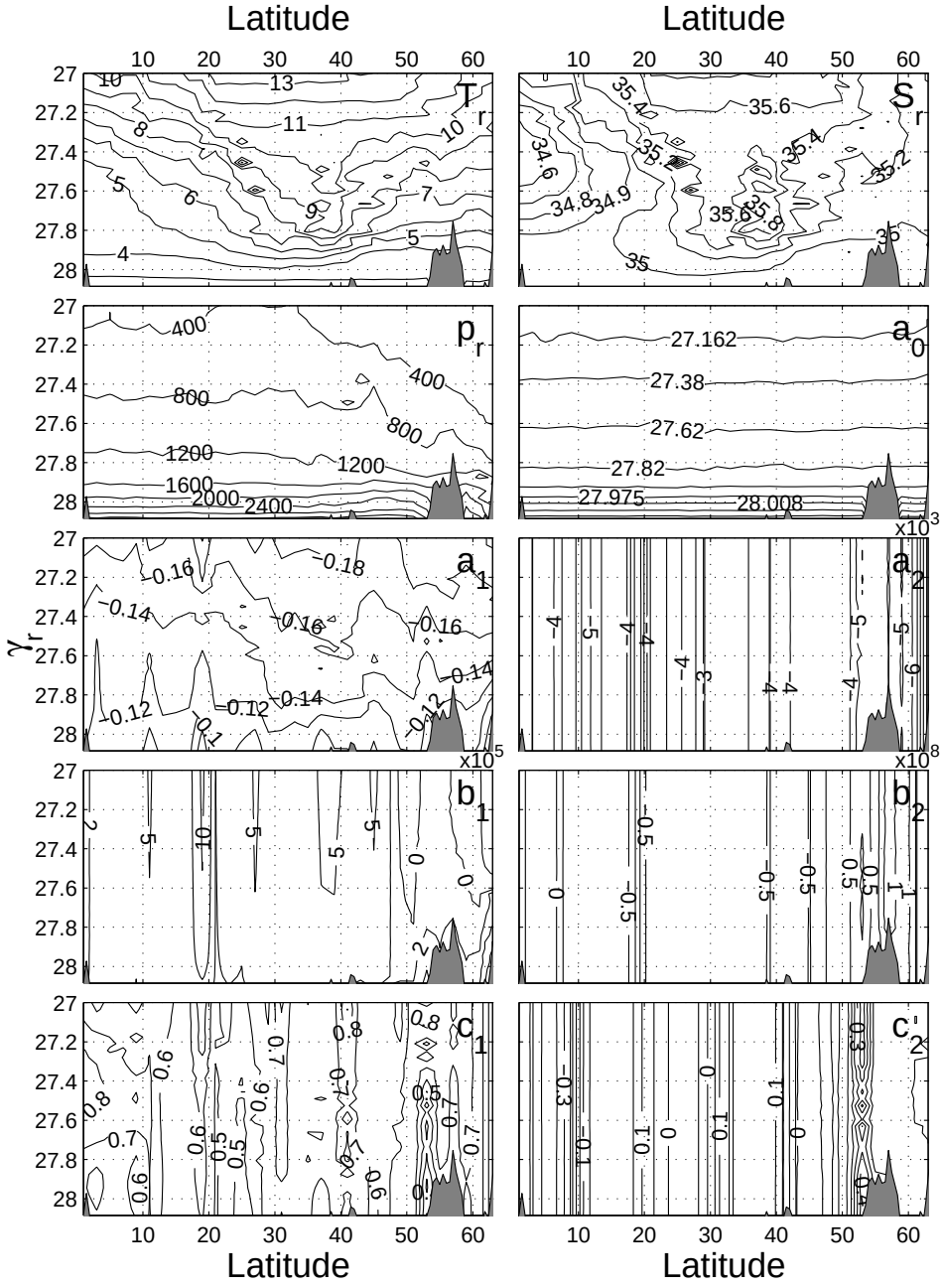

Figure 4: Reference values (θ_r, S_r, p_r) and polynomial coefficients (a_0, a_1, a_2, b_1, b_2, c_1, c_2) for density prediction, as a function of latitude and reference neutral-density (γ_r).

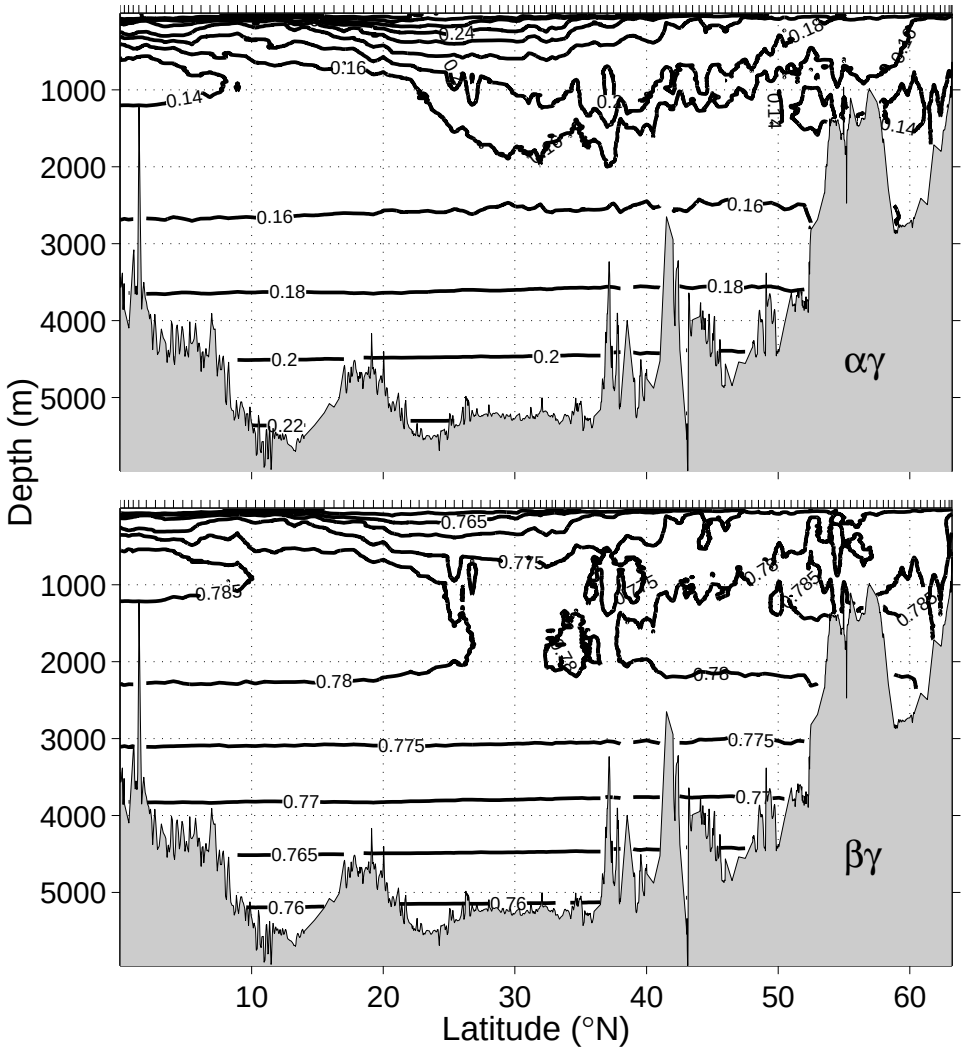

Figure 5: Thermal expansion $\alpha\gamma$ and salinity contraction $\beta\gamma$ distributions along the A16N WOCE section.

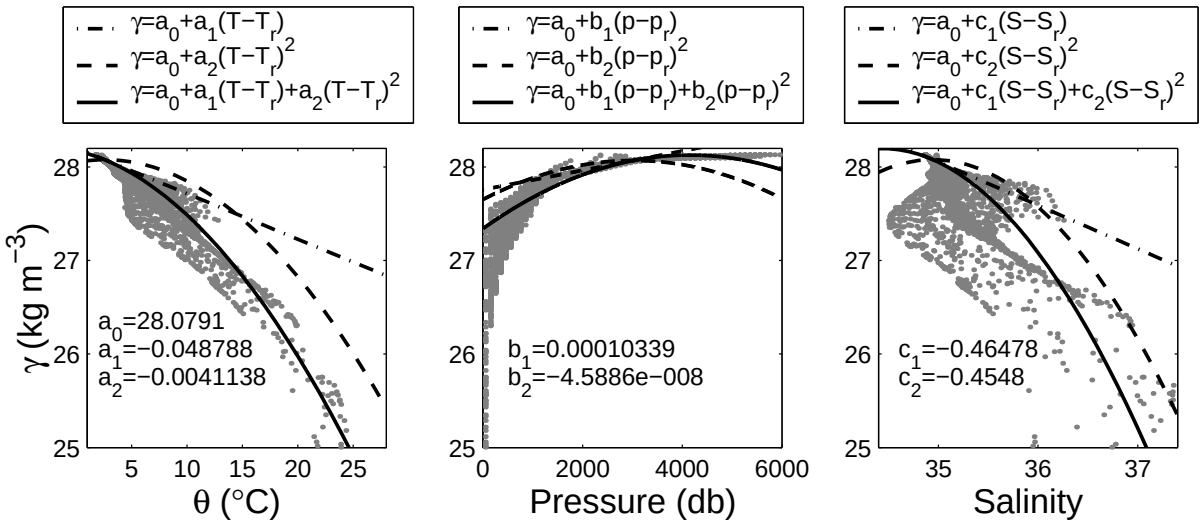

Figure 6: Property-property plots, with linear, quadratic and their sum superposed, as indicated in the upper legend (see text for details).

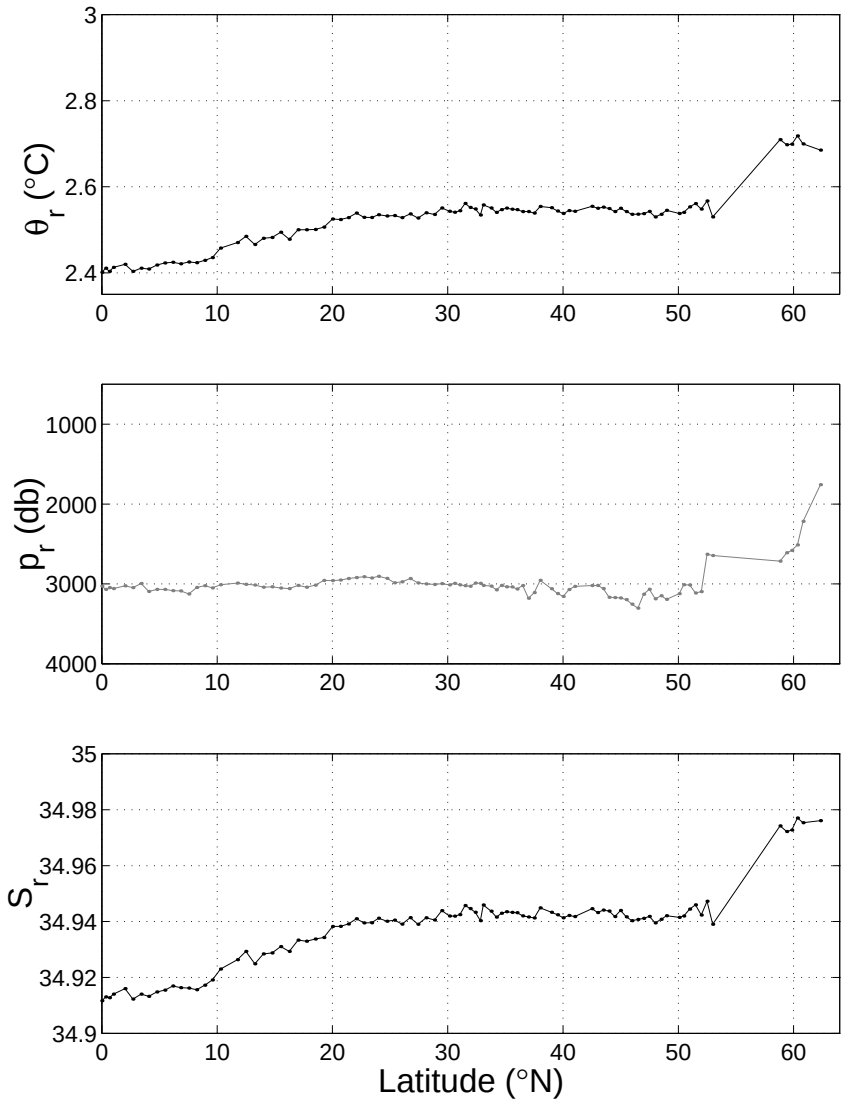

Figure 7: Latitudinal distribution of θ_r, p_r, S_r, for $\gamma_r = 28.072$.

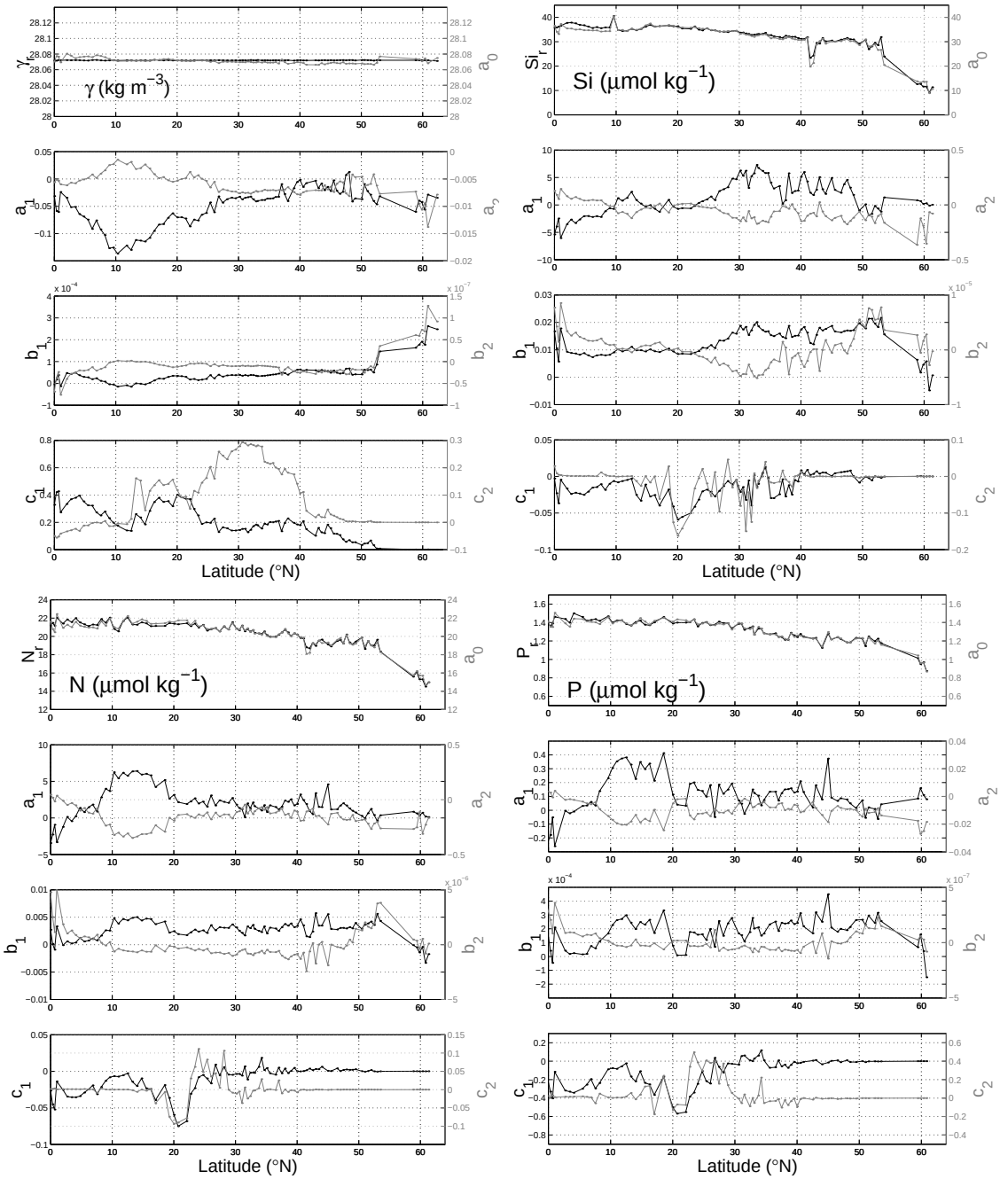

Figure 8: Meridional distribution of reference variables and coefficients for density γ, nitrate N, phosphate P, and silicate Si, for $\gamma_r = 28.072$.

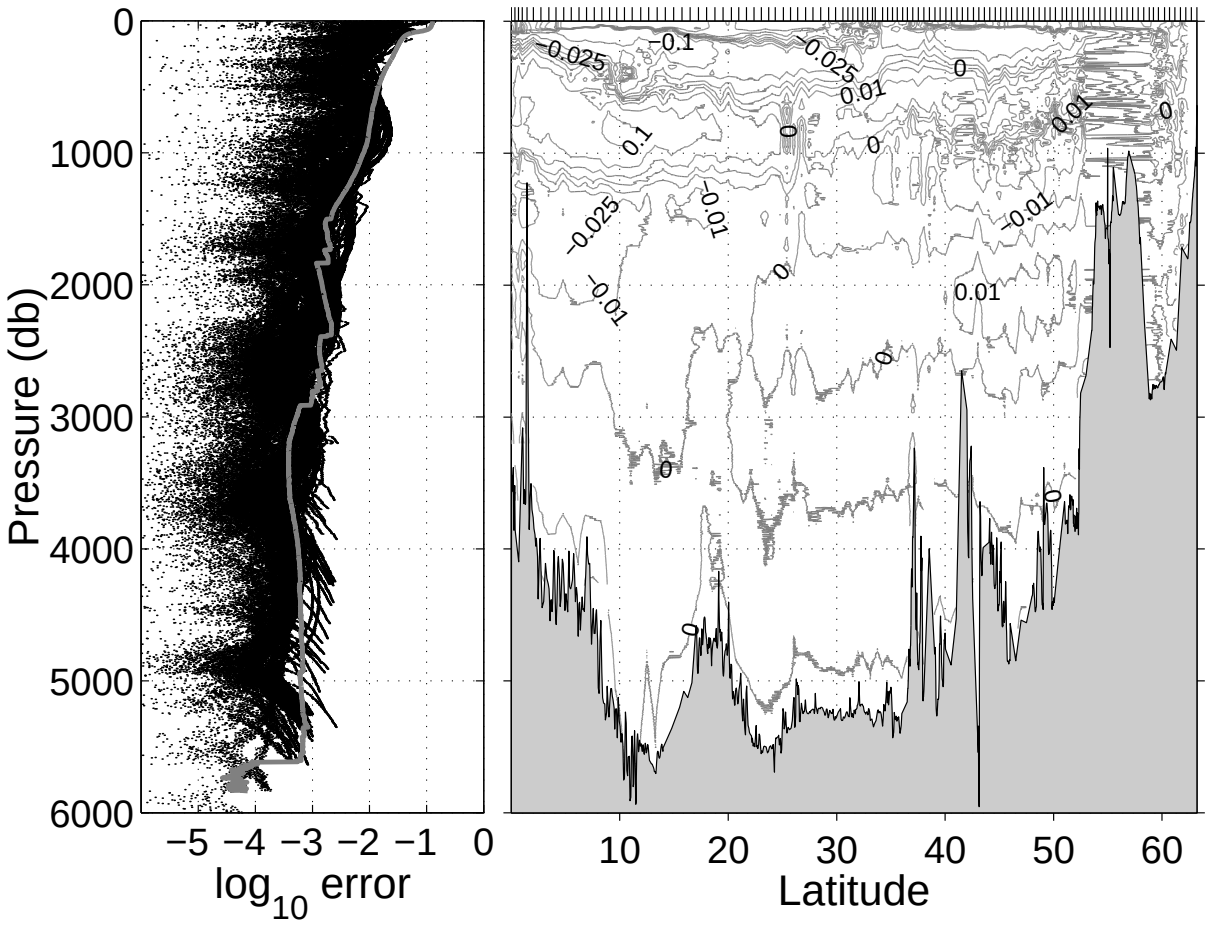

Figure 9: (Left) The solid line indicates the standard deviation in the density fluctuations and the dots show the errors in neutral-density prediction for all stations, as a function of pressure. (Right) Distribution of errors (kg m^{-3}) in neutral-density prediction along section A16N.

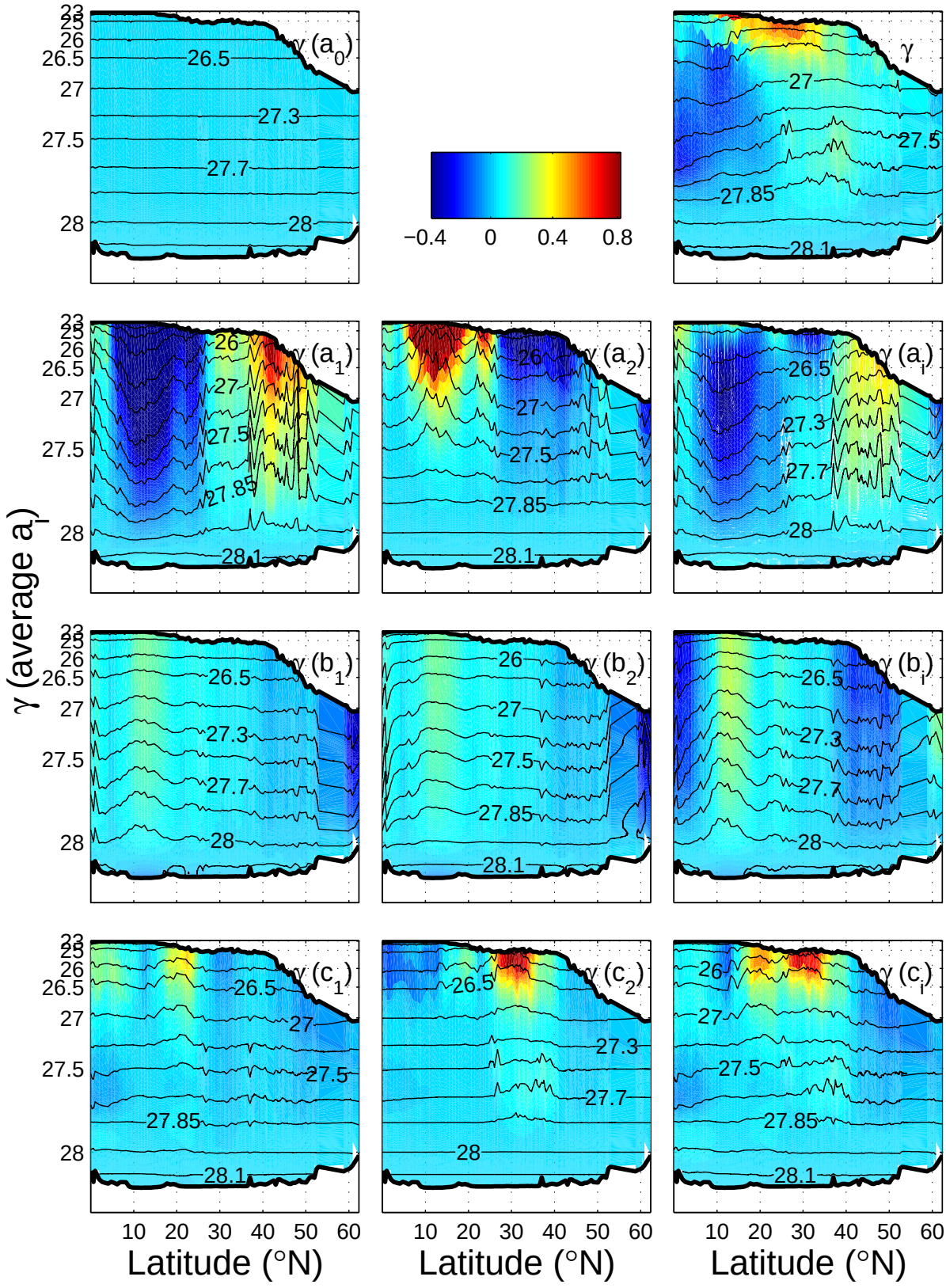

Figure 10: Meridional distribution of reconstructed density as a function of the mean reconstructed density and latitude (see text). Note the exponential scale in the vertical axes.

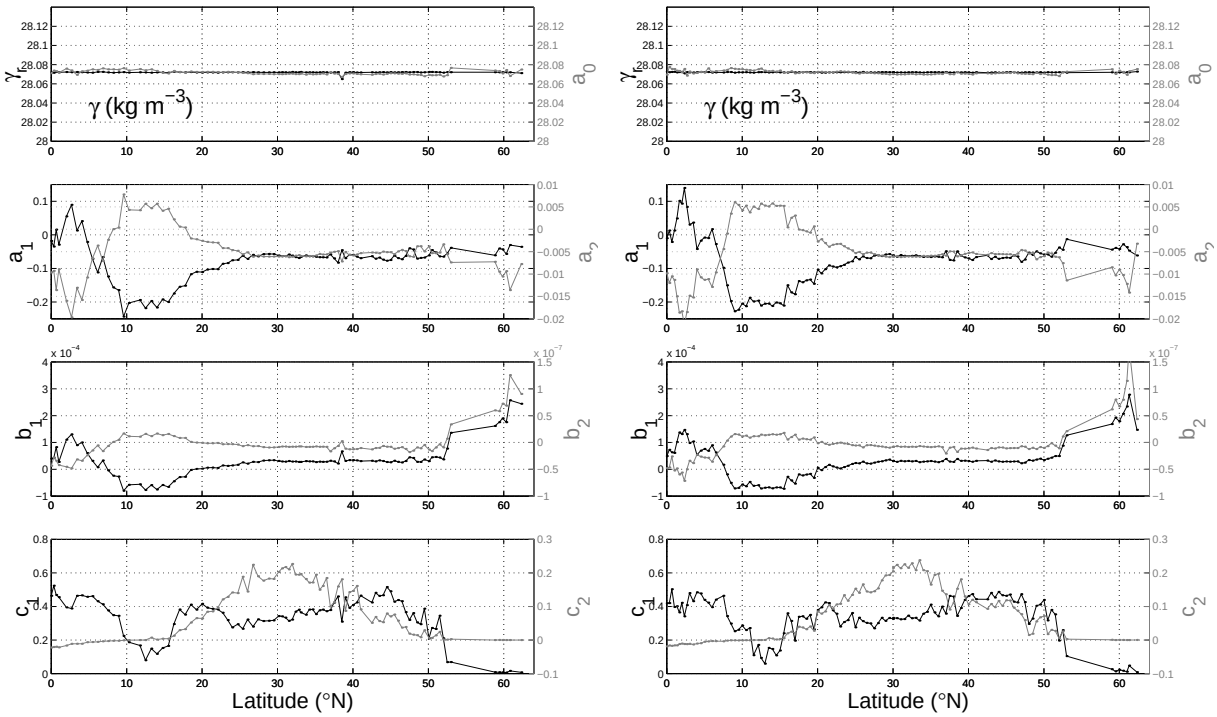

Figure 11: Meridional distribution of coefficients for density γ, as obtained for (left) the 1988 A16N section and (right) the 2003 homologous section, in both cases discarding observations with γ <26.85.

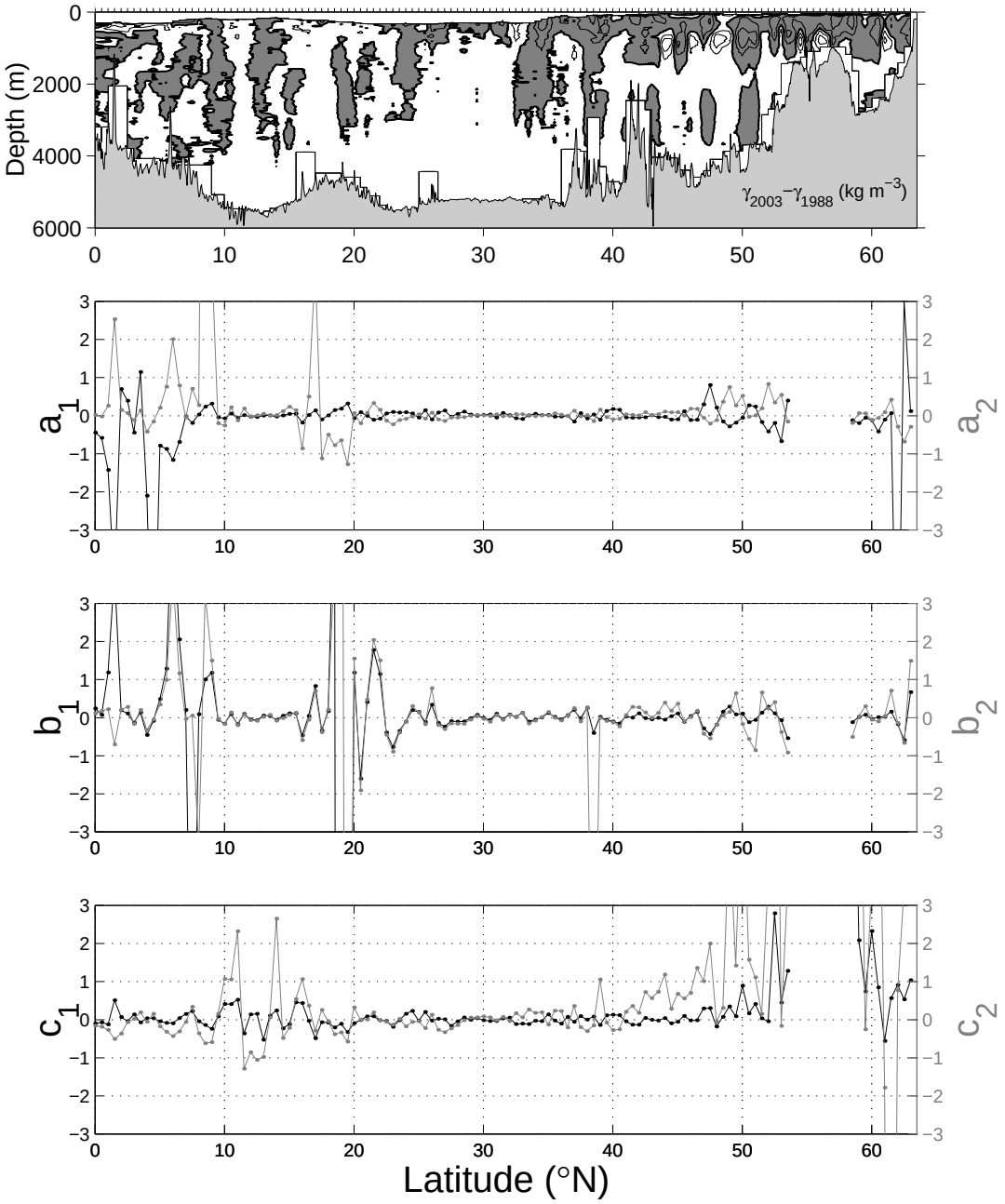

Figure 12: (Upper panel) Density differences between the 2003 and 1988 sections along section A16N. Shaded regions are negative values, the contours shown are -0.1, -0.05, 0, 0.05 and 0.1. (Remaining panels) Relative differences in coefficients between the 2003 and 1988 sections along section A16N. The fraction is calculated as the 2003 value less the 1998 value, divided by the latter, so a value of ± 1 implies a $\pm 100\%$ change in the 1998 coefficient.